Tidal energy resource characterisation in the Dover Strait by using VHF radar and ADCP measurements

Maxime Thiébaut, Alexei Sentchev

Progress in Renewable Energies Offshore – Guedes Soares (Ed.)
© 2016 Taylor & Francis Group, London, ISBN 978-1-138-62627-0

Tidal energy resource characterisation in the Dover Strait by using VHF radar and ADCP measurements

M. Thiébaut & A. Sentchev
Laboratory of Oceanology and Geosciences, UMR-CNRS 8187, ULCO, Wimereux, France

ABSTRACT: A methodology of tidal flow resource assessment in the eastern English Channel is presented. The study is performed using surface velocity time series recorded by VHF radars and ADCP velocity measurements. The most energetic area is located west of Cape Gris Nez with the peak velocity of 2.5 m/s, mean velocity of 1 m/s, and spring tide average velocity of 1.4 m/s. Velocities exceeding 1 m/s are observed more than 50% of time there. Averaged velocity profiles derived from ADCP data were obtained for different tidal stages and approximated by a power law function. Using velocity time series provided by the radars, the power law expression for velocity profiles and the power density time series in the surface and bottom layers were generated. The results show that the highest value of power density attains 0.9 kW/m^2 in the surface layer west of the Cape Gris Nez, with a peak value of 5 kW/m^2. In the rest of the domain, the mean power density varies from 0.1 to 0.6 kW/m^2.

1 INTRODUCTION

Converting tidal current kinetic energy into electric power by in-stream tidal turbines became a real challenge since the last years. The world tidal energy potential (tidal range and tidal current) is of the order of 3 TW (Charlier and Justus 1993), thus offering a significant source of renewable energy.

Sites with the biggest tidal stream potential are located on the northwest European shelf (Commission of the European Communities 1996) and in particular in the English Channel (?). Highly energetic areas such as Alderney Race, Bréhat Island region, Isle of Wight, and Dover Strait are considered as promising for tidal stream energy conversion (Commission of the European Communities 1996). Tidal projects are under development at several sites. In January 2016, the first 0.5 MW turbine was installed at Paimpol-Bréhat demonstration site in France. The new region Nord—Pas de Calais—Picardie has committed a sustainable development process with the purpose of dividing by 4 its gas emissions by 2050. Even if the tidal stream resource in the Dover Strait has been considered as non-negligible (?), there is no reliable estimate of the technically exploitable potential documented in scientific publications. The present study tendsto get the knowledge on resource distribution in the area.

Resource characterization is the first step towards a site selection and a turbine deployment planning (Blunden and Bahaj 2007). Two approaches can be followed to quantify the tidal stream potential in the most efficient way: extensive field measurements and numerical modelling.

Underway velocity measurements by a towed or vessel mounted ADCP (Acoustic Doppler Current Profiler) represent an efficient tool for tidal flow characterization and energy resource quantification (Gooch et al. 2009, Goddijn-Murphy et al. 2013). In the absence of spatial coverage with observations, point measurements of velocity by ADCP or Acoustic Doppler Velocimeter (ADV) offer a unique opportunity of resource quantification from in situ data (Thomson et al. 2012).

The resource quantification cannot be reduced to identification of regions with high current velocities. A wide range of factors have to be considered, especially temporal and spatial variability of the energy potential (Neill et al. 2014). Although, ADCP and ADV have shown their effectiveness, notably with the estimation of turbulence (Osalusi et al. 2009, Thomson et al. 2012) or to hydrodynamics models validation (Carballo et al. 2009), they do not turn out sufficient to the spatial coverage of a study area. In contrast, numerical modelling of coastal circulation appeared as a powerful tool for hydrokinetic potential mapping. It allowed a considerable improvement in the quality of velocity and available power estimation. Nowadays, 3D models are routinely applied for tidal energy site assessment, resource quantification, and studies of the impact of energy devices on the local circulation and environment (Lewis et al. 2015, Robins et al. 2015).

In this study, a technique of tidal flow resource assessment based on the analysis of surface current velocity time series recorded by Very High Frequency Radar (VHFR) (Sentchev and Yaremchuk 2007) in the Dover Strait is presented. Although the radar technology has been used in many oceanographic applications since more than 20 years (Paduan and Washburn 2013), its efficiency for tidal energy resource assessment was demonstrated only recently (Thiébaut and Sentchev 2015). Radar derived velocities are supplemented by current velocity profiles acquired by bottom mounted ADCPs in the study area. The radars allow continuous data acquisition of surface current velocities over a large area at high spatial and time resolution. ADCP data provide the comprehension of velocity variation with depth which is fundamental for tidal stream resource assessment.

2 DATA AND METHODS

2.1 *Study site, environmental conditions and constraints*

The study area is located in the Dover Strait (eastern English Channel), along the Opal coast of France (Figure 1, right panel). The coastline is meridionally oriented with a large embayment in the central part (Boulogne harbour) and a number of small inlets and river estuaries. The water depth is less than 50 m throughout the domain. In the middle of the Dover Strait, there are sandbanks oriented in the alongshore direction.

Investigation of the physical processes which govern the circulation along the Opal coast has been performed using VHFR observations (Sentchev and Yaremchuk 2007) and numerical modelling (Sentchev and Korotenko 2005, Du Bois et al. 2012, Jouanneau et al. 2013). The authors show that the local hydrodynamic is by far dominated by tidal motions. Remotely forced tidal wave determines the variability of the sea surface height (SSH) and currents in the study area. The SSH in the Boulogne Harbour (BLH) has a high range variations (4 to 9 m), whereas tidal current velocities have a typical magnitude of 1–1.5 m/s (Ouahsine et al. 2006). Currents are predominantly semi-diurnal with a pronounced fortnightly modulation due to the interference of the M_2, S_2 and N_2 tidal constituents. Asignificant asymmetry of the sea-surface elevation curve reveals a contribution of higher order nonlinear harmonics (M_4, MS_4). They also generate higher velocity during the flood flow compared to ebb flow (Korotenko and Sentchev 2011). Site assessment should take into account the environmental constraints relative to local economic activities. The Dover Strait is one

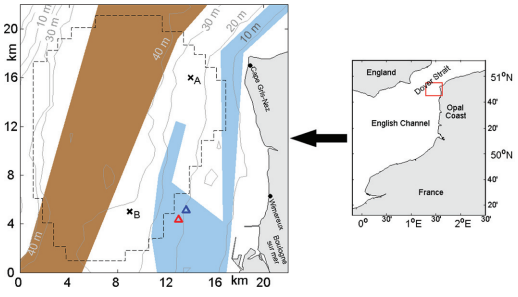

Figure 1. Experimental domain off the Opal coast in the eastern English Channel (red square contour on the right panel). Radar sites are shown by black dots and the blue and red triangles denotes the locations of ADCPs during the measurements performed in June 2008 and July 2009 respectively. Locations *A* and *B* (black crosses) have been selected for a detailed analysis. The brown domain shows the intensive east-west maritime traffic and the blue domain match the main fishing area. Contour interval of the bathymetry is 10 m (grey solid lines). Black dashed line indicate the radar coverage. Geographic names used in the text are also shown.

of the busiest seaways in the world. More than 400 commercial vessels cross the strait daily. The traffic safety is a critical issue because of high risk of collision in the strait. The navigation way of vessels travelling northward is shown by brown shading in Figure 1. The port of Boulogne is the biggest fishing port in France. Fishing is an important local economic activity and a large area is extensively exploited in the vicinity of the BLH (Figure 1, blue shading). These constraints particularly limit the area suitable for marine renewable energy exploiting.

Two particular locations not affected by constraints mentioned above, are chosen for further detailed analysis of the technically exploitable potential in the study area: northern and southern sectors of the radar coverage zone (Figure 1). They are not affected by constraints mentioned above. The water depth ranges from 25 to 35 m there which is favorable for tidal turbine installation (Couch and Bryden 2006).

2.2 *VHFR data*

In May–June 2003, two VHF radars were deployed to monitor surface currents off the French Opal coast for a 30-day period. One radar site was located on the Cape Gris Nez (hereafter Cape GN), 40 m above the sea level. The other radar was installed 12 km farther southward, in Wimereux (Figure 1). The VHFR system "COSMER" (?) measures the current velocity in the surface layer (0.7 m thick). The radars, operating at frequencies 45 MHz and 47.8 MHz, were configured to

provide measurements over a distance up to 25 km offshore at high spatial resolution: 600 m along beam and 10° azimuthal spacing, with time resolution of 20 minutes. The radial velocities measured by the two radars were interpolated on a regular grid with 1 km spacing. As a result, one month velocity time series were generated from May 1 to May 31, 2003. A detailed description of the experimental settings and methods of data processing of the radar network off the northern Opal coast can be found in (Sentchev and Yaremchuk 2007).

2.3 *ADCP data*

ADCP measurements from two 1.2 Mhz upward-looking four-beam broadband RDI ADCPs were used to supplement surface velocities provided by the radars. Both instruments were installed approximately 6 km west of the BLH, at 18 m mean depth (Figure 1). The first ADCP was deployed from 1 to 4 July 2008, during spring tide and the second one from 9 to 16 June 2009, covering the period of tide evolution from spring to neap. Velocities were recorded at 1 Hz in beam coordinates with 0.5 m vertical resolution, starting from 1 m above the bottom. The data from the surface 3 m thick layer were not considered in analyzed because of signal contamination by surface waves.

2.4 *Data analysis*

The Principal Component Analysis (PCA) (Thomson and Emery 2001) technique was applied to VHFR data set in order to quantify the tidal flow dynamics over the whole period of observations. Parameters of synthesized ellipses, retrieved from the PCA, provide two major properties of tidal currents, direction and magnitude, and also indicate the tidal flow anisotropy. The latter is estimated as the ratio of eigenvalues of the velocity correlation tensor. A rotary analysis technique was also applied to velocity time series (Thomson and Emery 2001) in order to identify the ellipse polarization or the sign of current vector rotation: positive for counterclockwise (ccw) rotation and negative for clockwise (cw) rotation. Other analysis methods, such as harmonic, spectral, and statistical analysis, were applied to both radar derived velocities and ADCP data.

2.5 *Metrics*

Current strength characterization involves an assessment of the maximum, time averaged velocity, and also asymmetry of the tidal flow. The mean velocity is the average of current velocity magnitudes over a long period including values around slack water. Moreover, the maximum sustained current velocity helps to establish design loads on device support structures and foundations.

Tidal flow asymmetry describes the difference between minimum and maximum of velocity magnitude. An imbalance between the strength of flood and ebb current can exist, generating a considerably more power production during a specific stage of the tide. The following expression was used to estimate the current asymmetry a:

$$a = < V >_{flood} / < V >_{ebl} \quad (1)$$

where brackets mean time averaging of the velocity magnitude on flood and ebb flow.

Surface current speed measured by VHFR used to assess the available resource at a site by estimating the power density for different tidal stage. As the VHFR measurements are particularly efficient for current monitoring, it is possible to evaluate the available power density at different spatial locations using the conventional formula:

$$P = 0.5\rho V^3 \quad (2)$$

where ρ is water density and V the current velocity.

VHFR data allows assessing only the surface current velocity. Generally the maximum velocities are observed near the surface and minimum values near the seabed. To determine a beneficial hub-height and optimize the turbine design, the knowledge of velocity profile is required. Velocity distribution in the water column is commonly approximated by the power law (Soulsby 1997):

$$V(z) = V_0(\frac{z}{d})^{1/\alpha} \quad (3)$$

V_0 is the surface velocity, d is the bottom depth, z is the distance above the seabed, and α is an empirical coefficient estimated from linear regression fit of LogLog representation of velocity. Using surface velocity time series provided by the radars, the power law expression for velocity profiles, the power density time series in the surface and bottom layers were produced.

3 RESULTS

3.1 *Tidal current velocity*

The parameters of synthesized tidal current ellipses used to quantify spatial variability of tidal currents derived from PCA are shown for 16 May 2003 (Figure 2). During this day, the strongest currents of spring tide were observed. Ellipse orientation

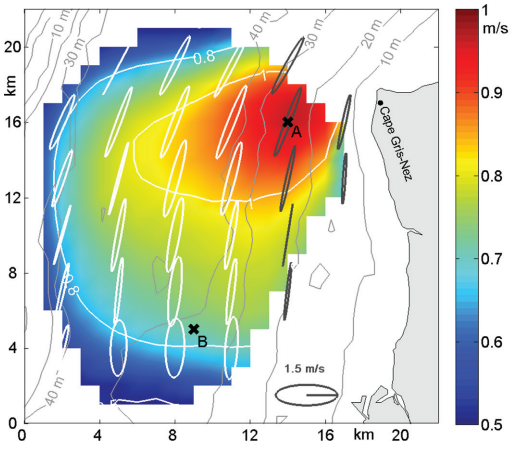

Figure 2. Mean surface current velocity during the whole study period (color shading) and during the spring tide period in May 2003 (white contours). Shown also tidal current ellipses derived from PCA on May 16, 2003 (every third ellipse is shown). Black ellipses denote counter-clockwise rotating tidal currents and white ellipses denote clockwise rotating currents. Black crosses show locations selected for detailed analysis.

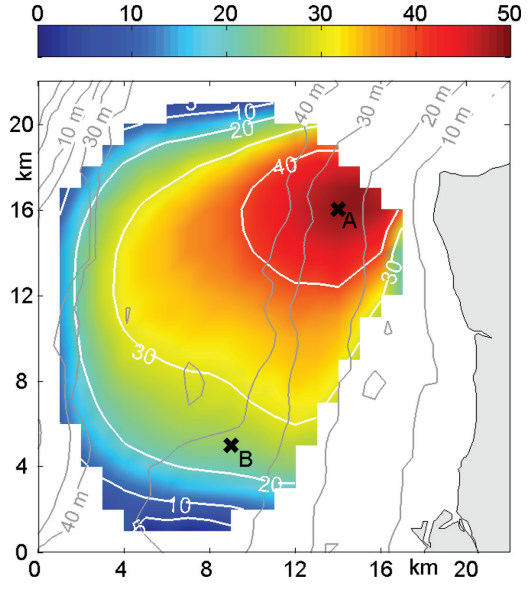

Figure 3. Percentage time current velocity of 1 m/s is exceeded.

shows that the current is strongly controlled by the topography, producing alignment of the major axes along the depth contours (Figure 2). An anisotropy in current field is observed with a relatively high ellipticity over the sandbanks, in the middle of the study domain.

White and black ellipses in Figure 2 indicate that the current are rotating clockwise (cw) and counter-clockwise (ccw) respectively. Two distinct zones with opposite sign of rotation of the tidal current vector are clearly identified. They are separated by a line roughly following the 30-m isobath. It suggests that in this location, tidal motion produces divergent (convergent) of surface currents during certain periods of the tidal cycle.

The time averaged current velocity varies from 0.5, on the perifery of the radar coverage zone, to 1 m/s, west of the Cape GN (Figure 2). The mean spring tide flow velocity shows similar spatial variations with the maximum value 1.2 m/s found offshore the Cape GN (Figure 2, white contour).

3.2 *Exceedance probability of velocity*

In tidal energy projects, it is customary to calculate the exceedance probability of velocity distribution: the percentage time of a specified current speed exceeded. Figure 3 shows spatial distribution of the percentage time of the current velocity of 1 m/s exceeded during the period of observation. Globally, the velocity value is reached in the majority of the domain with a minimum occurrence of 20%. In the central part, this velocity was exceeded 30% of time and in the northeastern sector, 50%of time.

Velocity histograms provide a simple way to evaluate the available resource at any point of a site. They indicate what percentage of time could be used for power generation. Figure 4 shows the cumulated occurrence of tidal current velocity observed in two locations selected for detailed analysis: point *A* located westward of the Cape GN and point *B* westward of the BLH (see Figure 3 for locations). The velocity of 1 m/s is exceeded 50% of time in location *A* and 25% of time in location *B*. The current speed of 1.5 m/s is exceeded 3 times more often in *A* than in *B* (respectively 18% and 6% of time). The mean current velocity is found to be 1 m/s in *A* and 0.75 m/s in *B*. This difference results from the change in flow regime. The strait narrowing and the presence of Cape GN cause flow acceleration and provides the highest tidal current velocity there.

3.3 *Flow asymmetry*

Tidal flow asymmetry basically concerns the asymmetry of velocity magnitude. A strong imbalance between the strength of flood and ebb current speeds can exist thus generating asymmetry in power extraction and reducing the overall energy yield (Neill et al. 2012).

The current asymmetry *a* is found higher than 1 in all the study domain (Figure 5), indicating the

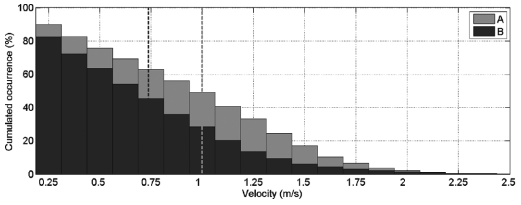

Figure 4. Cumulative occurrence of velocity magnitude in locations *A* and *B* (see Figure 3 for locations). Dashed lines represent the mean velocity at each site.

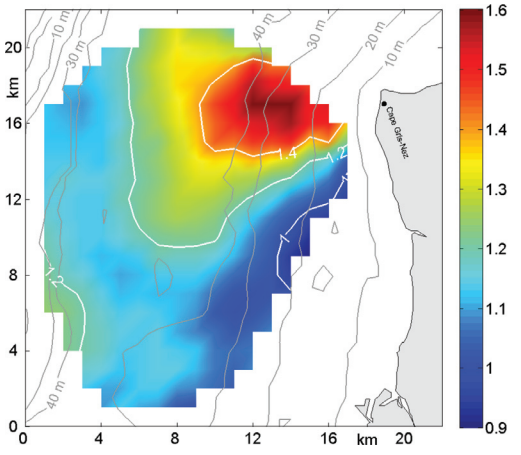

Figure 5. Current velocity asymmetry distribution.

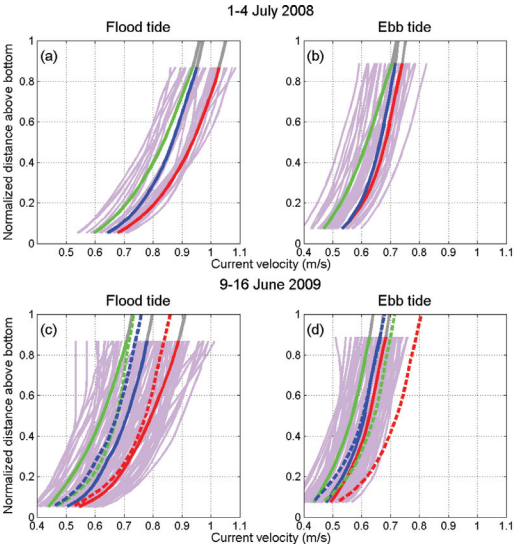

Figure 6. Current velocity profiles during flood and ebb tide flow derived from ADCP measurements in 2008 (a) and in 2009 (b). Mean velocity profiles during the peak current are shown in red (one hour averaging period is centered on peak velocity). One hour averaged velocity profiles observed one hour before and one hour after the peak velocity are given in green and blue respectively. Velocity profiles provided by ADCP (20-min averaged) are given in mauve. Only profiles with depth averaged velocity > 0.5 m/s are shown. Color solid and dashed lines match observed and modeled velocity profiles. Profile extrapolation to surface is shown in grey.

flood flow dominance. The only exception is the eastern part of the area with the asymmetry close to 0.9. The maximum current asymmetry ($a = 1.6$) is observed 6 km westward of the Cape GN, indicating the effect of cape on spatial distribution of phase and amplitude of the principal (M_2) tidal constituent and its higher order harmonics (M_4, MS_4) (Prandle 1993).

3.4 *Velocity profiles*

Knowledge of the variability of the flow with depth is a critical component of tidal energy resource assessment. Velocity profiles provided by ADCP measurements performed off the BLH, were analyzed for different stages of the tidal cycle: peak velocity period, flood and ebb flow period preceding and following the peak velocity. The time interval used for analysis was set to one hour for each tidal stage. The velocity profiles recorded during multiple 1-hour intervals were considered for each of the three tidal stages encountering the peak velocity. Figure 6 shows the time averaged velocity profiles observed during flood and ebb tidal flow.

Table 1. Power coefficient α approximated by a power law estimated from the best fit of the averaged velocity profiles over three periods around the peak velocity (P.V.). Standard deviation $\Delta\alpha$ estimated using individual 10-min averagedprofiles within all periods.

	P.V.–1h	P.V.	P.V.+1h	<α>	$\Delta\alpha$
Flood	5.6	6.1	6.5	6.0	1.1
Ebb	6	7.1	7.5	6.9	1

Based on the data acquired in 2008 and 2009, the vertical profile was found following a 1/6*th* law on flood tide and a 1/7*th* law on ebb tide. The analysis also shows that lower value of α is achieved one hour before the peak velocity. Then, it gradually increases until the maximum value, reached one hour after the peak velocity (Table 1). Moreover, *ha* shows larger variation on ebb tide than on flood tide with values ranging from 6 to 7.5 and 5.5 to 6.5 respectively (Table 1). The mean error of α estimation (standard deviation $\Delta\alpha$) for each 1 hour long stage of tidal flow was found to be close to 1.

3.5 *Tidal stream potential*

The kinetic power density is the primary metric used to characterize the theoretical potential and its spatial variation at a site. It is possible to evaluate the available power density at different space and time scales using the conventional formula for P (section 2.5). It was assumed that the ADCP-derived velocity profiles are representative for ebb and flood flow at each grid point within the study domain. Most of the tidal turbines are designed for deployment on the sea floor (e.g. Open Hydro, Sabella) but some of them (e.g. Hydro-Gen, Evopod by Oceanflow) are installed in the surface layer to take advantage of the highest current velocities. For this reason, the power density should be estimated for different altitudes according to device's deployment level. The power density time series in the surface and bottom layers (upper and lower half of the water column) were generated by assuming that the vertical variation of the current velocity follows a 1/6*th* and a 1/7*th* power law on flood and ebb flow respectively.

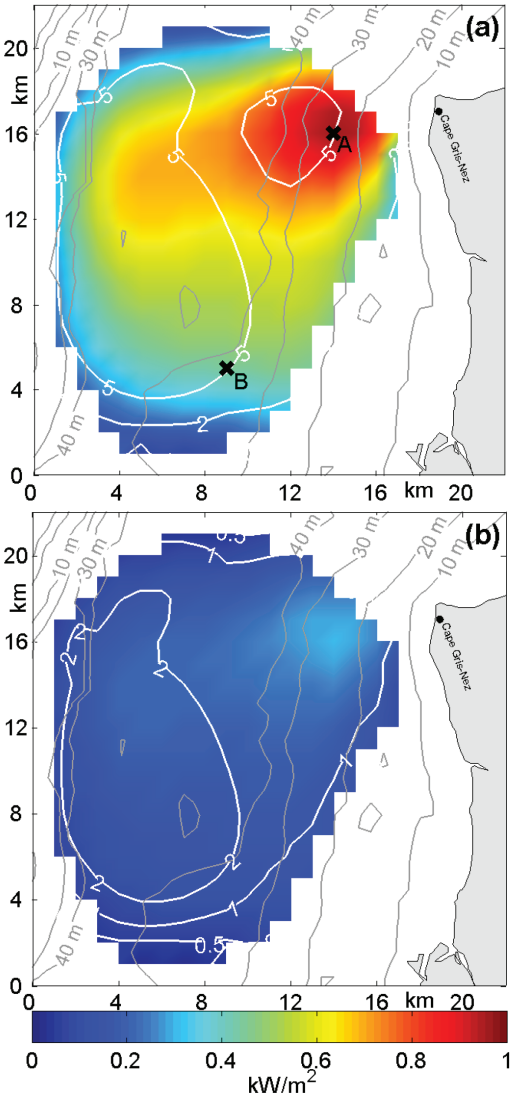

Figure 7. Maximum (white contours) and time averaged (color shading) kinetic power density available in the surface (a) and bottom (b) layers during the period of radar observations (May 2003).

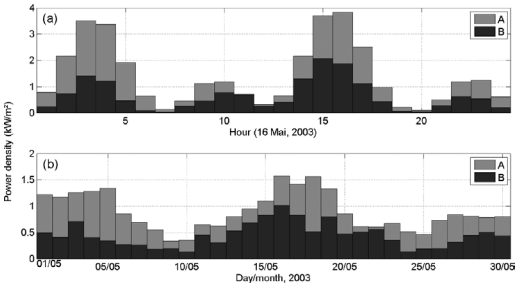

Figure 8. Hourly (a) and daily (b) values of power density in the surface layer in location A (grey) 748 and B (black).

As the only variable parameter governing the power is the current velocity, thus, it is not surprising to find similar spatial patterns for both mean tidal current velocity and mean kinetic power density distribution (color shading in Figure 2 and Figure 7). In the surface layer (Figure 7a) the mean power density attains 0.9 kW/m^2 in the northeastern sector, 5 km off the Cape GN, with peak values of 5 kW/m^2. For the rest of the study domain, the available power is much lower, with power density ranging from 0.1 to 0.6 kW/m^2. Offshore, even if the mean power available is 3 times lower than that estimated in the northern sector, peak power values are of the same order magnitude in both areas. In the bottom layer (Figure 7b), the highest power is also observed in northeastern sector, with the value of 0.3 kW/m^2 and the maximum value of 2 kW/m^2. On average, the kinetic power available in the bottom layer is 3 times lower than that available in the surface layer.

Figure 8 represents the hourly and daily values of P for two locations. A strong semi-diurnal variability is combined with a pronounced inequality of kinetic power in the surface layer caused by current asymmetry ($a = 1.6$ in location A and $a = 1.1$ in location B). Peak power during flood tide in location A and B, is respectively 3 and 2 times higher than that during ebb tide. For a month long period, a fortnight modulation of power is observed (Figure 8b). On average, the mean power available in location A exceeds that of in location B by a factor of two.

4 DISCUSSION

Two VHFR operating on the Opal coast of France in the eastern English Channel provided a 30-day long dataset of surface current velocities over an area of 500 km^2. Using advantages of the radar technology for remote sensing of coastal circulation (spatial coverage, high resolution, continuous data acquisition, …), the major metrics required for quantifying hydrokinetic resources of the tidal flow and their variation in time and space were estimated. VHFR derived surface velocities were supplemented by ADCP measurements performed 6 km offshore the port of Boulogne. This allowed quantifying the variability of hydrokinetic resources in three dimensions.

The area of high potential was found to be located westward of the Cape GN. There, the mean tidal current velocity is 1 m/s (Figure 2) with peak velocity of 2.5 m/s. The velocity of 1 m/s is exceeded 50% of time (Figure 3). Moreover, the tidal current asymmetry assessment shows that the majority of the domain is flood dominated ($a > 1$) with a maximum asymmetry value of 1.6 reached in the northeastern part of the area (Figure 5). The distortion of the tide is caused by the non-linear growth of compound tidal constituents (Aubrey and Speer 1985). Pingree and Griffiths (1979) have shown that the interaction of the principal semi-diurnal tidal current M_2 and its first harmonic, M_4, explains the general features of observed tidal asymmetries. Thiébaut and Sentchev (2015) showed that in the Fromveur Strait the spatial distribution of M_2 and M_4 phases are such that the current asymmetry varies in a wide range: from 0.5 to 2.5, generating high current velocity variation between flood and ebb tide. Numerical modelling of Jouanneau et al. (2013) revealed significant amplitude of M_4 along the Opal coast, generating a high asymmetry of the sea surface height there. The tidal current asymmetry can generate a significant variability of power production over a day thus reducing the overall energy yield (Neill et al. 2012).

Using ADCP measurements performed in July 2008 and June 2009, it was shown that the velocity profiles follow a power law. Analysis of the power coefficient α around the peak velocity was performed. The results revealed that α ranges from 6 to 7.5 and 5.5 to 6.5 for ebb and flood tide respectively. In each case the lowest value of α is achieved one hour before the peak velocity and the highest is reached one hour after the maximum current velocity.

Based on VHFR measurements, the mean kinetic power <*P*> in the surface layer, was estimated as 1 kW/m^2, in location *A*. For comparison the mean kinetic power in the more energetic region of the Alderney Race is of the order of 14 kW/m^2 (Coles et al. 2015). In the Fromveur Strait (Western Britanny), Thiébaut and Sentchev (2015) documented the mean power level of 5.5 kW/m^2. Regarding these resource assessments, it appears that the power available in the Dover Strait (location *A*) is low but not dramatically lower than that estimated at other sites considered as promising in European seas (Robins et al. 2015). The power estimation in the bottom layer demonstrated values three times lower than that assessed in the surface layer (Figure 8b). Combining equations (2) and (3), the expression of the vertical variation of power becomes:

$$P(z) = 12\rho V_0^3 (zd)^{3/\alpha} \quad (4)$$

Figure 9 shows the mean power profile for flood and ebb tide conditions. Power variation with depth takes into account the 1/6*th* and 1/7*th* power laws derived from statistic analysis of ADCP data (section 3.4). The mean depth-averaged power during both tidal conditions was estimated to be 0.7 kW/m^2 and 0.25 kW/m^2 on flood and ebb tide respectively, indicating the significant effect of the current asymmetry on available power. In order to evaluate the impact of α on power estimation, a 1/7*th* power law for velocity profiles was considered to generate the vertical variation of *P* during flood tide (dashed red curve in Figure 9). The 1/7*th* law provides overestimation of the depth-averaged power by 6% in comparison to the 1/6*th* law considered as the best fit of the vertical power variation on flood flow (solid red curve in Figure 9). This discrepancy increases in the lower half of the water column and achieves 11% on average.

The available practical power in the surface and bottom layers was estimated, considering the measured power curve of the twin-rotor Strangford Lough SeaGen MCT. The cut-in speed of this tidal turbine is 1 m/s and each drive train rates at 600 kW for current velocity higher than 2.3 m/s. Twin-rotor SeaGen turbines (16 m diameter *D*) was assumed to be installed in (a) the surface layer and (b) the bottom layer in an area of 1 km^2, centered on location *A*. Lateral and row spacing of tidal current generators were set to 3D and 30D respectively (Blunden, Bahaj, & Aziz 2013). Tidal array of 32 turbines arranged in two rows facing the principal flow direction was considered for available power calculation. In order to consider the reduction of incident flow speed on the second row downstream, a row-wise attenuation factor set to 0.9 was applied to the tidal current velocity (Blunden, Bahaj, & Aziz 2013). The annual tidal array power was estimated to be 23 GWh/km^2 and 9 GWh/km^2 in the surface and bottom layers respectively. Using hydrodynamic numerical model, Blunden et al. (Blunden, Bahaj, & Aziz

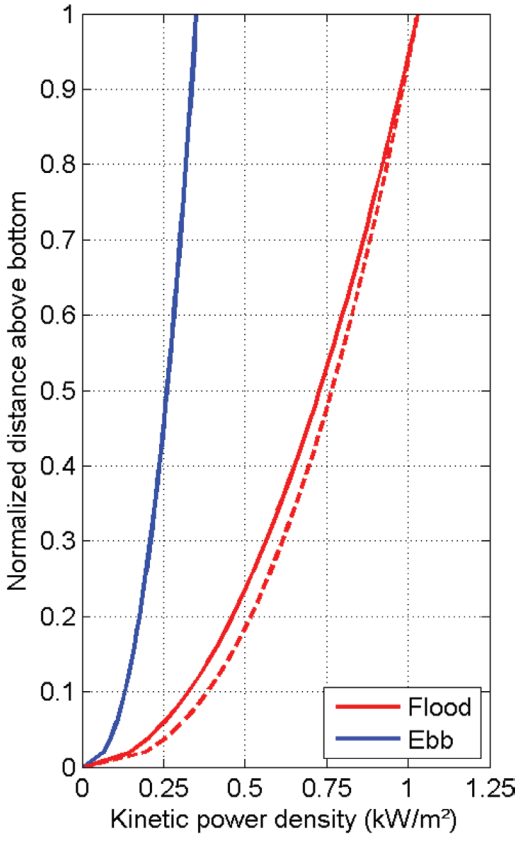

Figure 9. Vertical variation of kinetic power density in location *A* during averaged ebb and flood tide. Red dashed curve shows the vertical variation of *P* obtained during flood tide with a 1/7*th* power law.

2013) carried out tidal current power estimation in the Alas Strait, Indonesia. An area of approximately 30 km^2 (depth < 40 m) was selected as tidal turbine array. The complete array was assumed to consist of multiple sub-array, each selected grid cell (1 kmm^2 corresponding to the model resolution) was assigned on sub-array, consisting of 16–28 Seagen MCT turbines. By considering the depth-averaged current velocity and the downstream flow reduction in a tidal array, the annual energy yield was estimated to be 330 GWh, namely 11 GWh/km^2. This value is 25% lower than that estimated using the depth-averaged current velocity in location *A* (15 GWh/km^2).

5 CONCLUSIONS

In summary, surface velocity time series recorded by VHF radars were used for assessing circulation and mapping hydrokinetic resource in the Dover Strait in the eastern English Channel. The results showed that the most promising site for tidal turbine testing should be located 5 km westward of the Cape GN outside the corridor of the north-south maritime traffic and the main fishing area. The amount of power that could be generated is 3 times bigger during flood tide than during ebb tide. It is also found that the power decreases by a factor of 3 in the bottom layer compared to the surface layer. Based on ADCP measurements, the power coefficient α was determined during multiple 1-hour intervals, for each of the three tidal stages encountering the peak velocity. On average, the vertical variation of velocity with depth follows a 1/6*th* power law during flood tide and a 1/7*th* power law during ebb tide. Theses values were estimated with a standard deviation $\Delta\alpha = 1$. Variation of α within the accuracy range provides the power density variation of the order of 6%, for the depth averaged power, and 11% for power in the bottom layer. The available practical power considering a tidal array of 32 SeaGen turbines, arranged in two rows in an arrea of 1 km^2. The annual tidal array power was estimated to be 23 GWh/km^2 and 9 GWh/km^2 in the surface and bottom layers respectively.

ACKNOWLEDGMENTS

The study was supported by the project PROTIDE of the Interreg IVB NW Europe program and represents a contribution to this project. The authors acknowledge funding support by the PÃ´le Metropolitain de la CÃ´te d'Opale.

REFERENCES

Aubrey, D. G. & Speer, P. E. (1985). A study of non-linear tidal propagation in shallow inlet/estuarine systems Part I: Observations. *Estuarine, Coastal and Shelf Science 21*(2), 185–205.

Blunden, L. S. & Bahaj, A. S. (2007). Tidal energy resource assessment for tidal stream generators. *Proceedings of the Institution of Mechanical Engineers, Part A: Journal of Power and Energy 221*(2), 137–146.

Blunden, L. S., Bahaj, A. S. & Aziz, N. S. (2013). Tidal current power for Indonesia? An initial resource estimation for the Alas Strait. *Renewable energy 49*, 137–142.

Carballo, R., Iglesias, G. & Castro, A. (2009). Numerical model evaluation of tidal stream energy resources in the Ría de Muros (NW Spain). *Renewable Energy 34*(6), 1517–1524.

Charlier, R. H. & Justus, J. R. (1993). *Ocean energies: environmental, economic and technological aspects of alternative power sources*, Volume 56. Elsevier.

Coles, D. S., Blunden, L. S. & Bahaj A. (2015, September). Energy extraction potential from the Alderney Race.

Commission of the European Communities (1996). *The Exploitation of Tidal and Marine Currents: Wave Energy: Project Results*. European Commission.

Couch, S. J. & Bryden, I. (2006). Tidal current energy extraction: Hydrodynamic resource characteristics. *Proceedings of the Institution of Mechanical Engineers, Part M: Journal of Engineering for the Maritime Environment 220*(4), 185–194.

Du Bois, P. B., Dumas, F., Solier, L. & Voiseux, C. (2012). Insitu database toolbox for short-term dispersion model validation in macro-tidal seas, application for 2d-model. *Continental Shelf Research 36*, 63–82.

Goddijn-Murphy, L., Woolf, D. K. & Easton, M. C. (2013). Current patterns in the inner sound (Pentland Firth) from underway ADCP data*. *Journal of Atmospheric and Oceanic Technology 30*(1), 96–111.

Gooch, S., Thomson, J. Polagye, B. & Meggitt, D. (2009). Site characterization for tidal power. pp. 1–10. IEEE.

Jouanneau, N., Sentchev, A. & Dumas, F. (2013, December). Numerical modelling of circulation and dispersion processes in Boulogne-sur-Mer harbour (Eastern English Channel): sensitivity to physical forcing and harbour design. *Ocean Dynamics 63*(11–12), 1321–1340.

Korotenko, K. & Sentchev, A. (2011). Study turbulence in shallow tidal coastal zone. *Oceanology 51*, 1–14.

Lewis, M., Neill, S. P., Robins, P. E. & Hashemi, M. R. (2015). Resource assessment for future generations of tidal-stream energy arrays. *Energy 83*, 403–415.

Neill, S. P., Hashemi, M. R. & Lewis, M. J. (2014). The role of tidal asymmetry in characterizing the tidal energy resource of Orkney. *Renewable Energy 68*, 337–350.

Neill, S. P., Jordan, J. R. & Couch, S. J. (2012). Impact of Tidal Energy Converter (TEC) arrays on the dynamics of headland sand banks. *Renewable Energy 37*(1), 387–397.

Osalusi, E., Side, J. & Harris, R. (2009). Structure of turbulent flow in EMEC's tidal energy test site. *International Communications in Heat and Mass Transfer 36*(5), 422–431.

Ouahsine, A., Smaoui, H. & Senchev, A. (2006). Modelling of Tide and Tidally Induced Hydro-Sedimentary Processes in the Eastern Part of the English Channel. *Journal of Marine Environmental Engineering 8*(4).

Paduan, J. D. & Washburn, L. (2013). High-frequency radar observations of ocean surface currents. *Annual review of marine science 5,* 115–136.

Pingree, R. D. & Griffiths, D. K. (1979, May). Sand transport paths around the British Isles resulting from M2 and M4 tidal interactions. *Journal of the Marine Biological Association of the United Kingdom 59*(02), 497–513.

Prandle, D. (1993). Year-long measurements of flow-through the dover strait by HF radar and Acoustic Doppler Current Profilers (ADCP). *Oceanologica Acta 16*(5–6), 457–468.

Robins, P. E., Neill, S. P., Lewis, M. J. & Ward, S. L. (2015, June). Characterising the spatial and temporal variability of the tidal-stream energy resource over the northwest European shelf seas. *Applied Energy 147*, 510–522.

Sentchev, A. & Korotenko, K. (2005, November). Dispersion processes and transport pattern in the ROFI system of the eastern English Channel derived from a particle-tracking model. *Continental Shelf Research 25*(18), 2294–2308.

Sentchev, A. & Yaremchuk, M. (2007). VHF radar observations of surface currents off the northern Opal coast in the eastern English Channel. *Continental Shelf Research 27*(19), 2449–2464.

Soulsby, R. (1997). *Dynamics of Marine Sands: A Manual for Practical Applications*. London: Telford.

Thiébaut, M. & Sentchev, A. (2015). Estimation of Tidal Stream Potential in the Iroise Sea from Velocity Observations by High Frequency Radars. *Energy Procedia 76*, 17–26.

Thomson, J., Polagye, B., Durgesh, V. & Richmond, M. C. (2012). Measurements of turbulence at two tidal energy sites in Puget Sound, WA. *Oceanic Engineering, IEEE Journal of Oceanic Enginnering 37*(3), 363–374.

Thomson, R. E. & Emery, W. J. (2001). *Data analysis methods in physical oceanography*. Elsevier.